



Punch up your research!

Knockout cells for studying immune signaling pathways

InvivoGen



The Mitochondrial Phosphatase PGAM5 Is Dispensable for Necroptosis but Promotes Inflammasome Activation in Macrophages

This information is current as of May 11, 2017.

Kenta Moriwaki, Nivea Farias Luz, Sakthi Balaji, Maria Jose De Rosa, Carey L. O'Donnell, Peter J. Gough, John Bertin, Raymond M. Welsh and Francis Ka-Ming Chan

J Immunol 2016; 196:407-415; Prepublished online 18 November 2015;
doi: 10.4049/jimmunol.1501662
<http://www.jimmunol.org/content/196/1/407>

-
- Supplementary Material** <http://www.jimmunol.org/content/suppl/2015/11/18/jimmunol.1501662.DCSupplemental>
- References** This article **cites 39 articles**, 5 of which you can access for free at: <http://www.jimmunol.org/content/196/1/407.full#ref-list-1>
- Subscription** Information about subscribing to *The Journal of Immunology* is online at: <http://jimmunol.org/subscription>
- Permissions** Submit copyright permission requests at: <http://www.aai.org/About/Publications/JI/copyright.html>
- Email Alerts** Receive free email-alerts when new articles cite this article. Sign up at: <http://jimmunol.org/alerts>

The Journal of Immunology is published twice each month by The American Association of Immunologists, Inc., 1451 Rockville Pike, Suite 650, Rockville, MD 20852
Copyright © 2015 by The American Association of Immunologists, Inc. All rights reserved.
Print ISSN: 0022-1767 Online ISSN: 1550-6606.



The Mitochondrial Phosphatase PGAM5 Is Dispensable for Necroptosis but Promotes Inflammasome Activation in Macrophages

Kenta Moriwaki,^{*,1} Nivea Farias Luz,^{*,†,1} Sakthi Balaji,^{*} Maria Jose De Rosa,^{*,2} Carey L. O'Donnell,^{*} Peter J. Gough,[‡] John Bertin,[‡] Raymond M. Welsh,^{*} and Francis Ka-Ming Chan^{*}

The cytokine IL-1 β is intimately linked to many pathological inflammatory conditions. Mature IL-1 β secretion requires cleavage by the inflammasome. Recent evidence indicates that many cell death signal adaptors have regulatory roles in inflammasome activity. These include the apoptosis inducers FADD and caspase 8, and the necroptosis kinases receptor interacting protein kinase 1 (RIPK1) and RIPK3. PGAM5 is a mitochondrial phosphatase that has been reported to function downstream of RIPK3 to promote necroptosis and IL-1 β secretion. To interrogate the biological function of PGAM5, we generated *Pgam5*^{-/-} mice. We found that *Pgam5*^{-/-} mice were smaller compared with wild type littermates, and male *Pgam5*^{-/-} mice were born at sub-Mendelian ratio. Despite these growth and survival defects, *Pgam5*^{-/-} cells responded normally to multiple inducers of apoptosis and necroptosis. Rather, we found that PGAM5 is critical for IL-1 β secretion in response to NLRP3 and AIM2 inflammasome agonists. Moreover, vesicular stomatitis virus-induced IL-1 β secretion was impaired in *Pgam5*^{-/-} bone marrow-derived macrophages, but not in *Ripk3*^{-/-} bone marrow-derived dendritic cells, indicating that PGAM5 functions independent of RIPK3 to promote inflammasome activation. Mechanistically, PGAM5 promotes ASC polymerization, maintenance of mitochondrial integrity, and optimal reactive oxygen species production in response to inflammasome signals. Hence PGAM5 is a novel regulator of inflammasome and caspase 1 activity that functions independently of RIPK3. *The Journal of Immunology*, 2016, 196: 407–415.

The inflammatory cytokine IL-1 β plays critical roles in protective and pathological inflammation. Mature IL-1 β secretion requires two signals. The first signal involves

NF- κ B-dependent de novo synthesis of pro-IL-1 β . The second signal typically involves activation of a macromolecular signaling complex called the inflammasome, which consists of sensor proteins such as NLRP3 or AIM2, the adaptor protein ASC, and the IL-1 β converting enzyme/protease caspase 1 (1). Activation of the inflammasome and caspase 1 involves prion-like polymerization of the inflammasome (2, 3). Besides caspase 1, pro-IL-1 β processing can also be mediated by an alternative caspase 8 activating complex that contains receptor interacting protein kinase 1 (RIPK1), RIPK3, and FADD under certain conditions (4).

Recent discoveries have revealed key sentinel functions of the mitochondria in cell death and inflammation (5). Mitochondria-produced reactive oxygen species (ROS) and release of mitochondrial DNA have been implicated in inflammasome activation (6–8). PGAM5 was originally identified as a substrate of the E3 ligase cullin 3 through its binding to the adaptor Keap1 (9). PGAM5 promotes mitophagy (10, 11), a cellular process that eliminates damaged mitochondria. Furthermore, PGAM5 has been implicated in mitochondria fission through dephosphorylation and activation of the mitochondrial fission protein dynamin-related protein 1 (DRP1) (12). The RIPK3-PGAM5-DRP1 axis has been implicated to mediate death receptor- and oxidative stress-induced necrosis (12). In caspase 8-deficient bone marrow-derived dendritic cells (BMDCs), PGAM5 was reported to be involved in LPS-induced inflammasome activation and IL-1 β secretion (13). However, subsequent short hairpin RNA (shRNA) knockdown studies have challenged the role of PGAM5 in necroptosis and IL-1 β secretion (14–16).

To definitively evaluate the biology of PGAM5, we generated *Pgam5*-deficient mice. We found that male *Pgam5*^{-/-} mice were born at sub-Mendelian ratio. Moreover, surviving *Pgam5*^{-/-} mice were significantly smaller than their wild type littermates and continued to exhibit reduced viability into adulthood. Despite

^{*}Department of Pathology, University of Massachusetts Medical School, Worcester, MA 01605; [†]Centro de Pesquisas Gonçalo Moniz, Fundação Oswaldo Cruz, Universidade Federal da Bahia, Salvador-State of Bahia 40110-060, Brazil; and [‡]Pattern Recognition Receptor Discovery Performance Unit, Immuno-Inflammation Therapeutic Area, GlaxoSmithKline, Collegeville, PA 19422

¹K.M. and N.F.L. contributed equally to this work.

²Current address: Instituto de Investigaciones Bioquímicas de Bahía Blanca, Centro Científico Tecnológico-Bahía Blanca-Consejo Nacional de Investigaciones Científicas y Técnicas, Argentina.

ORCID: 0000-0002-2149-6127 (M.J.D.R.); 0000-0002-5110-9300 (P.J.G.); 0000-0002-4803-8353 (FK.-MC.).

Received for publication July 24, 2015. Accepted for publication October 22, 2015.

This work was supported by National Institutes of Health Grant AI083497 (to F.K.-M.C.), postdoctoral fellowships from the Uehara Memorial Foundation and the Japan Society for the Promotion of Science (to K.M.), and a fellowship from the National Council for Scientific and Technological Development (Brazil) (to N.F.L.).

K.M. and S.B. generated *Pgam5*^{-/-} mice; K.M. and M.J.D.R. characterized cell death in mouse embryonic fibroblasts and bone marrow-derived macrophages, respectively; N.F.L. characterized IL-1 β and reactive oxygen species production, and mitochondrial integrity; S.B. performed lacZ staining; C.L.O. and R.M.W. assisted with vesicular stomatitis virus infection; P.J.G. and J.B. provided critical reagents; and F.K.-M.C. conceived and supervised the project and wrote the paper.

Address correspondence and reprint requests to Dr. Francis Ka-Ming Chan, Department of Pathology, University of Massachusetts Medical School, AS9-1043, 368 Plantation Street, Worcester, MA 01605. E-mail address: francis.chan@umassmed.edu

The online version of this article contains supplemental material.

Abbreviations used in this article: BMDC, bone marrow-derived dendritic cell; BMDM, bone marrow-derived macrophage; CCCP, carbonyl cyanide 3-chlorophenylhydrazone; DRP1, dynamin-related protein 1; MEF, mouse embryonic fibroblast; RIPK1, receptor interacting protein kinase 1; ROS, reactive oxygen species; shRNA, short hairpin RNA.

Copyright © 2015 by The American Association of Immunologists, Inc. 0022-1767/15/\$30.00

these growth and survival defects, *Pgam5*^{-/-} cells responded normally to multiple inducers of apoptosis and necroptosis. Rather, we found that *Pgam5*^{-/-} bone marrow-derived macrophages (BMDMs) were highly impaired in inflammasome activation and mature IL-1 β secretion. PGAM5 stimulates inflammasome independent of RIPK3, because *Ripk3*^{-/-} and *Ripk3* kinase inactive BMDMs did not exhibit the same defect in IL-1 β secretion. In response to inflammasome activation, *Pgam5*^{-/-} BMDMs underwent extensive reduction in mitochondrial volume and produced reduced level of ROS. In wild type BMDMs, PGAM5 translocated to the same detergent-insoluble compartment in which the inflammasome adaptor ASC resides upon stimulation with LPS and the NLRP3 inflammasome agonist nigericin. Moreover, LPS and nigericin induced PGAM5 oligomerization within this detergent-insoluble compartment. Strikingly, oligomerization of the inflammasome adaptors was severely impaired in *Pgam5*^{-/-} BMDMs. These results established PGAM5 as a novel regulator of inflammasome activity that functions independently of RIPK3.

Materials and Methods

Generation of *Pgam5*-deficient mice

Targeted ES cell clone JM8.N4 (EPD0226_5_H02) was obtained from the European Conditional Mouse Mutagenesis Program. Proper recombination was confirmed by Southern blot (Supplemental Fig. 1A, 1B). The ES cells were injected to C57BL/6J-Tyr[c-2J]/J (albino-B6) to generate chimeric mice in transgenic animal core at University of Massachusetts Medical School. Germline transmission of the lacZ allele was confirmed by Southern blot. To generate *Pgam5*^{fl/+} mice, we crossed *Pgam5*^{lacZ/+} mice with the flippase transgenic mice (Gt(ROSA)26Sor^{tm1(FIP)Dym}). To generate *Pgam5*^{-/-} mice, we crossed *Pgam5*^{fl/+} mice with mice expressing Cre under the *Sox2* gene promoter. The excision of lacZ/Neo cassette and exon 2 was confirmed by Southern blot. Timed pregnancy test was set up with *Pgam5*^{-/-}*Fadd*^{+/-} intercrosses to determine rescue of embryonic lethality of *Fadd*^{-/-} mice. The embryos were fixed in 0.2% glutaraldehyde, 2% formalin, 5 mM EGTA, and 2 mM MgCl₂ in 0.1 M phosphate buffer (pH 7.3). After rinsing with 0.1% sodium deoxycholate, 0.2% IGEPAL CA-630 (Sigma), 2 mM MgCl₂ in 0.1 M phosphate buffer (pH 7.3) for three times, 20 min each, the embryos were stained with 1 mg/ml X-gal in potassium ferricyanide and potassium ferrocyanide (5 mM each) dissolved in the rinse solution for overnight at 37°C. The embryos were washed two times with 1 \times PBS, 15 min each the next day. All animal experiments were approved by the institutional animal care and use committee.

Cell culture

To generate BMDMs, we cultured 2B1J cells in DMEM containing 10% FBS, antibiotics, and 20% L929-conditioned medium for 7 d. BMDCs were generated by culture of BM cells in RPMI 1640 supplemented with 10 ng/ml GM-CSF and 5 ng/ml IL-4 for 7 d. *Asc*^{-/-}, *Casp1*^{-/-}, *Tnfr1*^{-/-}, *Tlr4*^{-/-}, *Myd88*^{-/-}, *Trif*^{-/-}, and *Ripk1*^{-/-} J2 virus-transformed macrophages were cultured in DMEM containing 10% FBS and antibiotics. Wild type and *Pgam5*^{-/-} mouse embryonic fibroblasts (MEFs) were cultured in DMEM containing 10% FBS and antibiotics. *Pgam5*^{-/-} MEFs were transduced with retrovirus carrying SV40 large T Ag/pMSCV and subsequently selected for hygromycin B resistance. SV40-immortalized *Pgam5*^{-/-} MEFs were lentivirally transduced with wild type *Pgam5* isoform 1, isoform 2, and the phosphatase dead mutant (H104A)pTRIPZ. Transduced cells were selected for puromycin resistance. HepG2 liver cancer cells were transduced with lentivirus expressing shRNA against the *Pgam5* gene (#1, V3LHS_312914; #2, V2LHS_62587; Open Biosystems) and subsequently selected for puromycin resistance. Nonsilencing shRNA (RHS4346; Open Biosystems) was used as a control. No sex difference was observed with BMDMs and BMDCs generated from male or female mice.

Measurements of IL-1 β secretion

BMDMs were plated a day before stimulation. After 3-h stimulation with 200 ng/ml ultrapure LPS (Invivogen), BMDMs were treated with silica (40 μ g/ml), nigericin (10 μ M) or ATP (5 mM) for another 3 h. Poly dA: dT (1 μ g/ml) is transfected into cells using Lipofectamine 2000 as per manufacturer's instructions. *N*-acetyl cysteine and carbonyl cyanide 3-chlorophenylhydrazone (CCCP) were obtained from Calbiochem and Sigma, respectively. For vesicular stomatitis virus (VSV) infection,

BMDMs were primed with 100 ng/ml LPS for 4 h. After incubation with VSV (Indiana strain, propagated in BHK21 cells, multiplicity of infection = 5) for 2 h, cells were further incubated for 4 h before supernatants were harvested. For in vivo IL-1 β secretion, 5-wk-old mice were injected with LPS (20 μ g/kg) and 700 μ g Alum Imject Adjuvant (Thermo Scientific) in 200 μ l PBS i.p. Peritoneal exudates were obtained with 700 μ l PBS containing 1% FBS 2 h after injection. IL-1 β secretion in the culture supernatants or the exudates was assessed by ELISA (BD Biosciences).

Quantitative PCR

Total RNA from various organs of 7-wk-old mice or BMDMs was used for reverse transcription followed by real-time PCR as described previously (17). *Pgam5* gene expression level in tissues was normalized to the average expression of the two housekeeping genes *Tbp* and *Hprt*. Cytokine expression was normalized to that of *Tbp*. The following primers were used: 5'-TGCCAATGTCATCCGCTAT-3' and 5'-GGTGATACTGCCGTTGTTGA-3' for *Pgam5*; 5'-CAAACCCAGAATTGTTCTCCTT-3' and 5'-ATGTGGTCTTCTGAAATCCCT-3' for *Tbp*; 5'-TGAAGAGCTACTGTAATGATCAGTCAAC-3' and 5'-AGCAAGCTTGCAACCTTAACCA-3' for *Hprt*; 5'-CCCACTGGTACATCAGCAC-3' and 5'-TCTGCTCATTACAGAAAGG-3' for *Il1b*; 5'-CCCACTCTGACCCCTTTACT-3' and 5'-TTTGAGTCCTTGATGGTGGT-3' for *Tnf*; 5'-CGGAGAGGAGACTTCACAGA-3' and 5'-CCAGTTTGGTAGCATCCATC-3' for *Il6*; and 5'-AGGTGTCCCAAGAAGCTGTA-3' and 5'-ATGCTGGACCCATTCCTTCT-3' for *Mcp1*.

Western blotting

Whole-cell extracts were prepared from various organs of 6-wk-old mice or cells using radioimmunoprecipitation assay buffer supplemented with protease inhibitor mixture (Roche). For BMDMs, whole-cell lysates were prepared with standard 1% Nonidet P-40 lysis buffer. For chemical cross-linking, cells were treated with 100 ng/ml LPS for 3 h, followed by 25 μ M zVAD-fmk for 30 min before stimulation with 10 μ M nigericin for 30 min. Cells were lysed in 1% Nonidet P-40, 150 mM NaCl, 20 mM Hepes (pH 7.5) supplemented with protease and phosphatase inhibitor cocktails (Sigma). After centrifugation at 1800 rpm, supernatant was removed and the insoluble pellet fraction was centrifuged at 5000 rpm and washed with CHAPS buffer [20 mM Hepes (pH 7.5), 5 mM MgCl₂, 0.5 mM EDTA, 0.1% CHAPS] before chemical cross-linking with 4 mM disuccinimidyl suberate (Life Technologies). Reaction was stopped after 30 min with Tris-Cl (pH 7.4). Western blotting was performed with Abs against ASC (N-15; Santa Cruz), caspase 1 (M-20; Santa Cruz), Caspase 8 (1G12; Enzo Life Sciences), PGAM5 (ab126534; Abcam), IL-1 β (AF-401-NA; R&D Systems), Tom20 (13929; Cell Signaling Technology), Drp1 (8570; Cell Signaling Technology), phopsho-Drp1 Ser637 (4867; Cell Signaling Technology), β -actin (3779; Prosci), and HSP90 (68/Hsp90; BD Biosciences) Abs.

Cell death assay

Cells were pretreated with 10 μ M z-VAD-fmk, 0.2 μ M BV6, and/or 10 μ M Nec-1 for 1 h before stimulation with TNF or LPS. Hydrogen peroxide (Sigma), rotlerin (Enzo Life Sciences), thapsigargin (Sigma), staurosporine (Enzo Life Sciences), and ABT737 (ApexBio) were used for cell death induction. PGAM5 expression was induced for 24 h by 1 μ g/ml doxycycline (Sigma) before stimulation. Cell death was determined by FACS using propidium iodide and FITC-Annexin V (BD Biosciences), CytoTox96 Non-Radioactive Cytotoxicity Assay, CellTiter 96 Aqueous One Solution Cell Proliferation Assay, or CellTiter-Glo Luminescent Cell Viability Assay (Promega).

Measurement of ROS and mitochondria

Intracellular ROS was detected with the specific fluorescent probe CM-H₂DCFDA (Molecular Probes). BMDMs were primed with 200 ng/ml LPS for 2.5 h, then loaded with 10 μ M CM-H₂DCFDA at 37°C for 30 min, exposed to 10 μ M nigericin, and further incubated for 30 min. After washing twice with PBS, the cells were analyzed using LSRII (BD Biosciences). For mitochondria morphology, BMDMs were stained for 30 min with 250 nM MitoTracker Red (Invitrogen) and DAPI (Enzo Life Science). Images were captured using a Leica Microsystems confocal microscope with a 63 \times objective. For the quantification of mitochondrial surface and volume, the 3D Object counter plugin for the Fiji software (version 2.0) was used (18). In brief, we used the distance in pixels, the physical distance of the image, and a pixel aspect ratio of 1 to define the pixel size in micrometers. After defining the threshold between signal and background, the volume and surface of the MitoTracker channel is calculated through the image slices.

Statistical analysis

All assays were performed in triplicates and the results represent mean \pm SEM. The *p* values were calculated with unpaired *t* test with Welch's correction. The *p* values <0.05 are considered statistically significant.

Results

Impaired growth and survival of *Pgam5*^{-/-} mice

We generated *Pgam5* mutant mice in which the β -galactosidase gene was inserted into the *Pgam5* locus (*Pgam5*^{lacZ/lacZ}; Supplemental Fig. 1A, 1B). β -Galactosidase staining of *Pgam5*^{lacZ/lacZ} embryos revealed that *Pgam5* was highly expressed in the whole epiblast at embryonic day 7.5 (Supplemental Fig. 1C). In adult mice, PGAM5 expression could be detected in multiple tissues by quantitative PCR and by Western blot (Fig. 1A, 1B). However, residual expression of *Pgam5*, especially in the brain, was still detected in *Pgam5*^{lacZ/lacZ} mice (Fig. 1A). To fully inactivate *Pgam5*, we first crossed *Pgam5*^{lacZ/lacZ} mice to flippase transgenic mice to remove the lacZ cassette, followed by breeding with Sox2-Cre deleter transgenic mice to delete exon 2 of *Pgam5* (Supplemental Fig. 1A, 1B). Western blot confirmed that *Pgam5*^{-/-} MEFs and *Pgam5*^{-/-} mice lack PGAM5 expression (Fig. 1B, Supplemental Fig. 1D). Unexpectedly, we found that male *Pgam5*^{-/-} mice, but not female *Pgam5*^{-/-} mice, were born at sub-Mendelian ratio (Fig. 1C). *Pgam5*^{-/-} mice were smaller and exhibited reduced body weight compared with their wild type littermates at weaning age (Fig. 1D, Supplemental Fig. 1E). Consistent with an early growth and survival defect, *Pgam5*^{-/-} mice had a higher mortality rate within the first 100 d (Fig. 1E). These results suggest that PGAM5 is required for optimal growth and organismal survival.

PGAM5 is dispensable for cell death by multiple inducers

PGAM5 was identified as a downstream RIPK3 substrate in necroptosis (12), although more recent studies showed that shRNA knockdown of *Pgam5* did not significantly affect TNF-induced necroptosis (14, 15). To evaluate whether the growth phenotype of *Pgam5*^{-/-} mice is caused by changes in cell death, we tested the response of *Pgam5*^{-/-} cells to various cell death inducers. We found that wild type and *Pgam5*^{-/-} primary MEFs treated with TNF, z-VAD-fmk, and the Smac mimetic BV6 exhibited similar levels of necroptosis (Fig. 2A). However, because different batches of primary MEFs exhibited a wide range of sensitivity to necroptotic and apoptotic inducers (Supplemental Fig. 2A–C), we

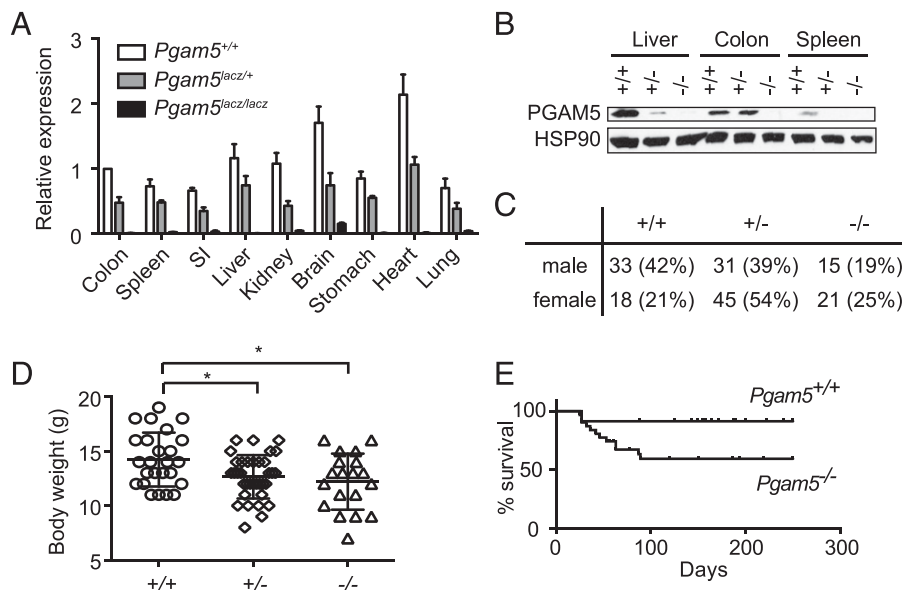
generated SV40-immortalized *Pgam5*^{-/-} MEFs and reconstituted the cells with lentivirus expressing PGAM5 in a doxycycline-inducible manner. Induction of the two wild type mouse PGAM5 isoforms, which differ in a single amino acid residue (Fig. 2B), as well as the phosphatase inactive PGAM5 mutant H104A (19), did not affect TNF-, z-VAD-fmk-, and BV6-induced necroptosis compared with mock-transduced MEFs (Fig. 2C). In addition, TNF and BV6-induced apoptosis was also not affected by expression of PGAM5 (Fig. 2D). Moreover, apoptosis induced by the kinase inhibitor staurosporine or the Bcl-2 inhibitor ABT737 was also independent of PGAM5 expression (Supplemental Fig. 2D).

PGAM5 was reported to mediate oxidative stress-induced cell death (12). Contrary to this report, we found that expression of wild type or H104A PGAM5 in *Pgam5*^{-/-} MEFs did not alter cell death induced by hydrogen peroxide, the mitochondrial uncoupler rottlerin, and the endoplasmic reticulum stress inducer thapsigargin (Supplemental Fig. 2E). In addition, we found that shRNA-mediated knockdown of PGAM5 did not protect HepG2 cells from acetaminophen-induced cell death (Supplemental Fig. 2F), a process reported to be mediated by ROS and RIPK3 (20).

In macrophages, LPS and z-VAD-fmk induced necroptosis independent of the inflammasome or autocrine TNF production, but nonetheless required the TLR4 adaptors TRIF and MyD88 and RIPK1 kinase activity (Supplemental Fig. 3A–C). Consistent with their roles in necroptosis, *Ripk1*^{-/-} and *Ripk3*^{-/-} BMDMs were refractory to LPS and z-VAD-fmk-dependent necroptosis (Fig. 2E) (21). By contrast, *Pgam5*^{-/-} and wild type BMDMs responded similarly to LPS and z-VAD-fmk-induced necroptosis (Fig. 2E). Collectively, the results in Fig. 2 indicate that PGAM5 is dispensable for cell death triggered by classical apoptosis and necroptosis inducers.

Necroptosis can be induced through mechanisms beyond TNFR1 and TLR4. For example, FADD or caspase 8 deficiency compromised survival of developing embryos through RIPK1- and RIPK3-dependent necroptosis (22–24). However, this event was delayed, but not abrogated, by inhibiting TNFR-1 or TRIF signaling (25, 26), indicating that developmental necroptosis involves death receptor- and TLR3/4-independent mechanisms. To test the potential role of PGAM5 in developmental necroptosis, we set up timed pregnancy test with *Pgam5*^{-/-} *Fadd*^{+/-} mice. At weaning age, no *Pgam5*^{-/-} *Fadd*^{-/-} mice were recovered from *Pgam5*^{-/-} *Fadd*^{+/-} intercrosses (Table I). Moreover, the few *Pgam5*^{-/-}

FIGURE 1. *Pgam5*^{-/-} mice are born at sub-Mendelian ratio and exhibit reduced body weight. **(A)** *Pgam5* expression from various tissues of 7-wk-old mice was determined by real-time PCR. **(B)** PGAM5 protein expression in the indicated tissues was determined by Western blot. **(C)** Male *Pgam5*^{-/-} mice were born at sub-Mendelian ratio. The number of progenies from *Pgam5*^{+/-} intercrosses with the indicated genotypes was shown. The percentages are shown in parentheses. **(D)** *Pgam5*^{-/-} mice exhibit reduced body weight. Body weight of mice with the indicated genotypes from *Pgam5*^{+/-} intercross was determined on day 28 after birth. *Pgam5*^{+/+} (*n* = 25), *Pgam5*^{+/-} (*n* = 35), *Pgam5*^{-/-} (*n* = 19). Bars represent mean \pm SEM. **p* \leq 0.01. **(E)** *Pgam5*^{-/-} mice exhibit increased mortality. *Pgam5*^{+/+} (*n* = 22), *Pgam5*^{-/-} (*n* = 30). SI, small intestine.



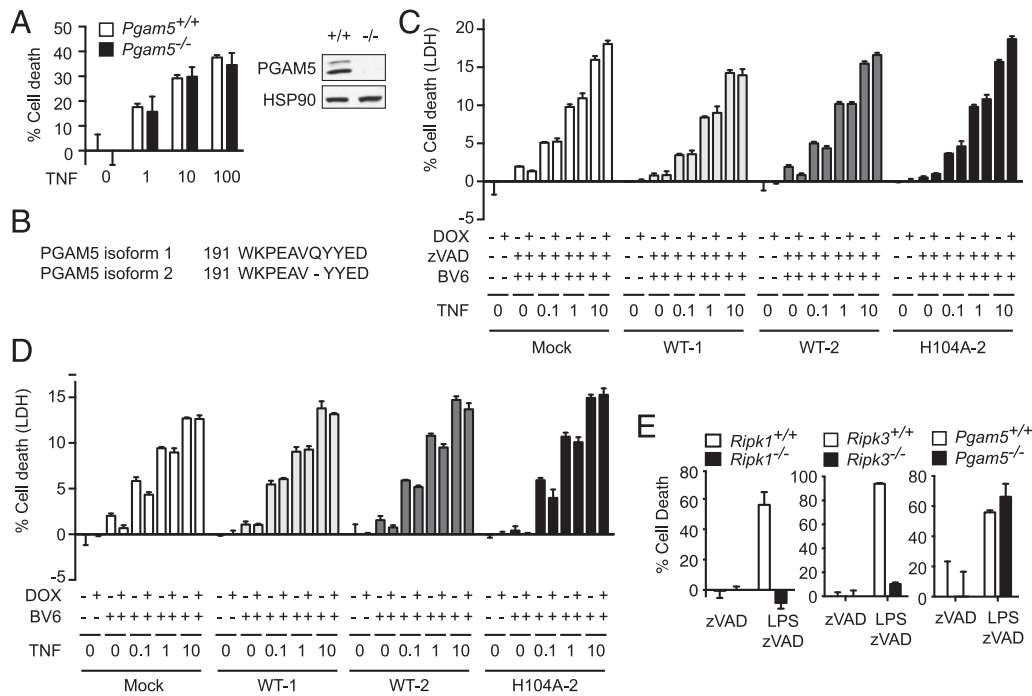


FIGURE 2. PGAM5 is dispensable for necroptosis and apoptosis. **(A)** Primary MEFs were stimulated with the indicated amount of TNF (ng/ml), 10 μ M z-VAD-fmk (zVAD), and 0.2 μ M BV6 for 24 h. Western blot shows that PGAM5 expression was abolished in *Pgam5*^{-/-} MEFs. **(B)** Sequence alignment of mouse PGAM5 isoform 1 and 2 shows that the two isoforms differ in a single glutamine residue that is absent in isoform 2. **(C and D)** SV40-transformed *Pgam5*^{-/-} MEFs transduced with PGAM5 wild type isoform 1 (WT-1), isoform 2 (WT-2), or phosphatase-dead mutant of isoform 2 (H104A-2) were stimulated with indicated amount of TNF (ng/ml) in the presence of 0.2 μ M BV6 and/or 10 μ M zVAD. **(E)** *Ripk1*^{-/-} and *Ripk3*^{-/-} J2 virus-transformed macrophages and *Pgam5*^{-/-} BMDMs were stimulated with 100 ng/ml LPS and 10 μ M zVAD for 12 h. Cell death was determined as described in *Materials and Methods*. Results shown are mean \pm SEM.

Fadd^{-/-} embryos that were detected between embryonic days 10.5 and 13.5 were highly deformed (data not shown). Hence we conclude that PGAM5 is dispensable for developmental necroptosis.

PGAM5 promotes optimal IL-1 β secretion

In caspase 8-deficient BMDMs, LPS stimulation led to exaggerated IL-1 β processing and mature IL-1 β secretion in an RIPK3-dependent manner. Knockdown of *Pgam5* expression by shRNA ameliorated the heightened IL-1 β secretion by caspase 8-deficient BMDMs (13), suggesting that PGAM5 participates in pro-IL-1 β maturation. In contrast, a recent report showed that although RIPK3 is required for pro-IL-1 β processing in response to infection by negative strand RNA viruses, shRNA knockdown of PGAM5 did not inhibit RNA virus-induced pro-IL-1 β processing (16). To investigate the role of PGAM5 in pro-IL-1 β processing, we primed *Pgam5*^{fl/fl} or *Pgam5*^{-/-} BMDMs with LPS, followed by stimulation with the NLRP3 inflammasome agonists silica, nigericin, ATP, or the AIM2 inflammasome agonist poly(dA:dT). Surprisingly, *Pgam5*^{-/-} BMDMs produced reduced level of IL-1 β in response to all inflammasome agonists (Fig. 3A, Supplemental Fig. 3D). Time-course analysis showed that nigericin-induced IL-1 β secretion by *Pgam5*^{-/-} BMDMs was reduced at all time points tested (Fig. 3B), indicating that the deficiency was not due to delayed response of *Pgam5*^{-/-} BMDMs. In contrast with BMDMs, *Pgam5*^{-/-} BMDCs are largely normal for IL-1 β secretion

(Fig. 3C). The differential requirement of PGAM5 for IL-1 β secretion in BMDMs was not caused by differences in cell death, because LPS or LPS and nigericin induced a similar level of cell death in *Pgam5*^{-/-} BMDMs and BMDCs compared with their *Pgam5*^{fl/fl} counterparts (Fig. 3D). Although mature IL-1 β secretion was reduced in *Pgam5*^{-/-} BMDMs, *Il1b* mRNA expression, as well as that of *Tnf*, *Mcp1*, and *Il6*, was normal in *Pgam5*^{-/-} BMDMs (Fig. 3E). These results suggest that PGAM5 does not regulate cytokine gene transcription, but rather participates in pro-IL-1 β processing. Indeed, reduced level of cleaved active caspase 1 was detected in nigericin-treated *Pgam5*^{-/-} BMDMs (Fig. 3F). In contrast, caspase 8, which has been shown to participate in pro-IL-1 β processing in certain conditions (17, 27, 28), was not activated in *Pgam5*^{fl/fl} and *Pgam5*^{-/-} BMDMs (Fig. 3F). These results indicate that PGAM5 promotes pro-IL-1 β processing through caspase 1-associated inflammasome rather than the recently described RIPK1-RIPK3-FADD-Caspase 8 complex (4).

Inflammasome activation is achieved through polymerization of the complex (2, 3). This process can be measured by isolating the detergent-insoluble fractions from cells and chemical cross-linking to capture higher-order ASC oligomers (29). In wild type BMDMs, nigericin-driven ASC oligomerization was detected concomitant with appearance of cleaved caspase 1 (Fig. 3G). In contrast, translocation of ASC to the insoluble compartment and

Table I. Number of progenies of each genotype from *Pgam5*^{-/-}*Fadd*^{+/-} intercrosses

	<i>Pgam5</i> ^{-/-} <i>Fadd</i> ^{+/+}	<i>Pgam5</i> ^{-/-} <i>Fadd</i> ^{+/-}	<i>Pgam5</i> ^{-/-} <i>Fadd</i> ^{-/-}
E10.5–13.5	11	20	5
D28	12	25	0

E, embryonic day.

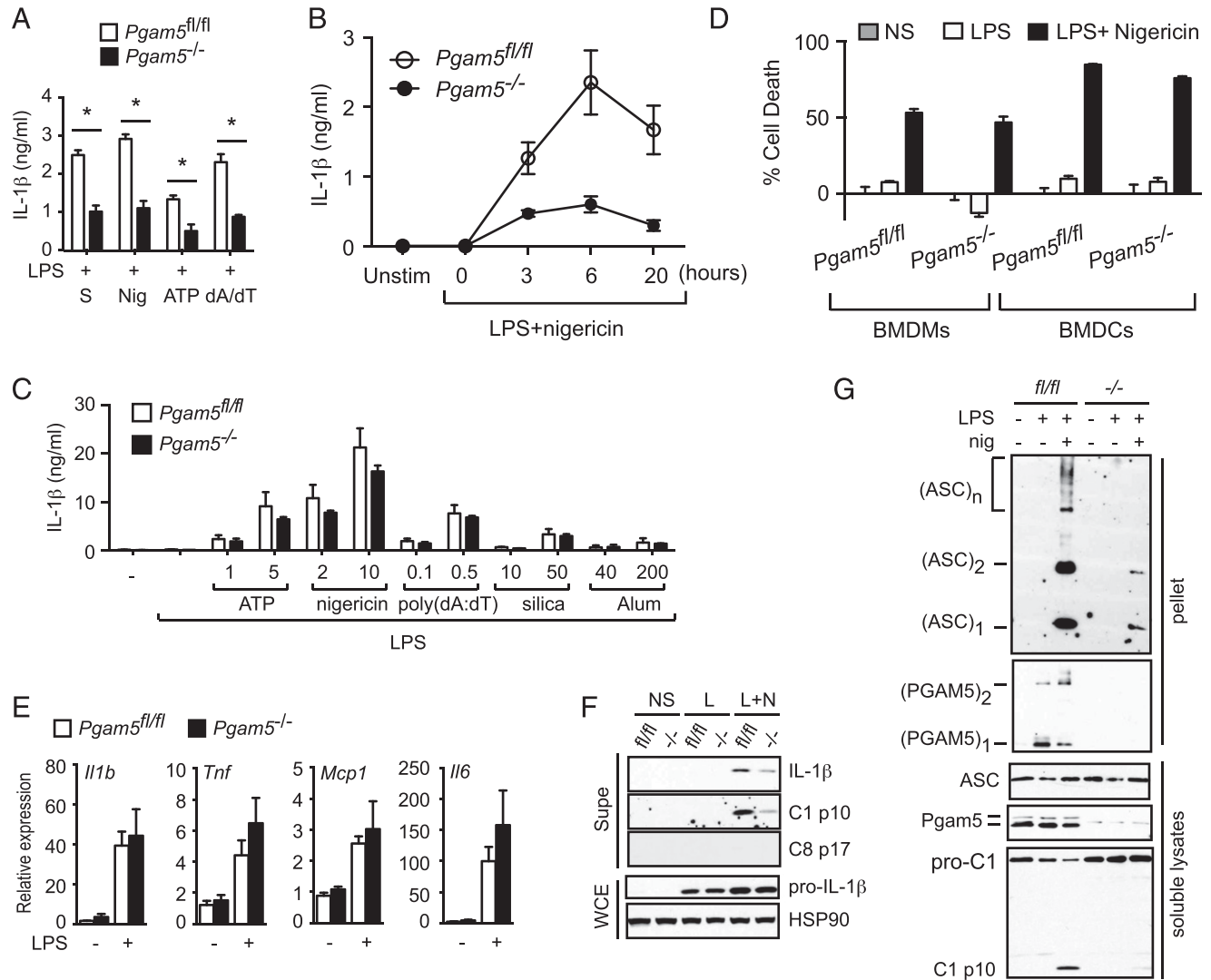


FIGURE 3. PGAM5 is required for optimal caspase 1 activation and IL-1 β secretion. **(A)** LPS-primed BMDMs were stimulated with the silica (S), nigericin (Nig), ATP, or poly(dA:dT) (dA/dT) for 3 h. IL-1 β secretion was determined by ELISA. **(B)** Kinetic measurements of IL-1 β secretion by LPS-primed BMDMs treated with nigericin for the indicated amount of time. **(C)** PGAM5 is dispensable for IL-1 β secretion in BMDCs. BMDCs were primed with 10 ng/ml LPS for 3 h and the indicated concentrations of ATP (mM), nigericin (μ M), silica (μ g/ml), alum (μ g/ml), or poly(dA:dT) (μ g/ml) for another 3 h before ELISA detection of secreted IL-1 β in the culture media. **(D)** PGAM5 deficiency did not affect cell death induced by LPS or LPS + nigericin in BMDMs and BMDCs. Cells primed with 200 ng/ml LPS for 3 h were stimulated with 10 μ M nigericin for 3 h. Cell death was determined by CellTiter-Glo Luminescent Cell Viability Assay. **(E)** BMDMs were stimulated with LPS for 3 h, and cytokine expression was determined by quantitative PCR. **(F and G)** *Pgam5*^{fl/fl} or *Pgam5*^{-/-} BMDMs were stimulated with LPS (L) for 3 h, followed by 10 μ M nigericin (N) for 30 min. Whole-cell extracts (WCE) or supernatants (Supe) were subjected to Western blot (F). The detergent insoluble fraction was subjected to chemical cross-linking as described in *Materials and Methods* (G). Monomers, dimers, and oligomers of ASC and PGAM5 were shown (G). Results shown are mean \pm SEM. **p* \leq 0.05.

ASC oligomerization was severely blunted in *Pgam5*^{-/-} BMDMs (Fig. 3G). Moreover, LPS induced translocation of PGAM5 to the detergent-insoluble compartment and PGAM5 oligomerization, which was further enhanced by nigericin treatment [Fig. 3G, compare (PGAM5)₂ with (PGAM5)₁]. Hence in response to LPS and nigericin, PGAM5 translocates to a detergent-insoluble compartment and undergoes oligomerization to facilitate inflammasome activation.

PGAM5 sustains mitochondrial integrity and ROS production

PGAM5 is a mitochondrial phosphatase that has been implicated to regulate mitochondrial homeostasis (10, 11, 30–32). Consistent with the notion that it is a positive regulator of mitochondrial fission, the mitochondria in *Pgam5*^{-/-} BMDMs appeared to be elongated (Fig. 4A, top panels and white arrow in inset). This is confirmed when mitochondrial surface and volume were quantified

by confocal microscopy (Fig. 4B). However, expression of mitochondrial proteins such as Tom20 and Drp1 was not changed in *Pgam5*^{-/-} BMDMs (Supplemental Fig. 1D). LPS treatment led to fragmentation of the mitochondria and a concomitant reduction in mitochondrial surface and volume in *Pgam5*^{-/-}, but not *Pgam5*^{fl/fl} BMDMs (Fig. 4A, middle panels and insets, 4B). Nigericin treatment of LPS-stimulated *Pgam5*^{fl/fl} BMDMs led to fragmentation of the mitochondria. In contrast, nigericin did not further increase mitochondrial fragmentation in *Pgam5*^{-/-} BMDMs (Fig. 4A, bottom panels and insets). These results suggest that the mitochondria in *Pgam5*^{-/-} BMDMs are more susceptible to signal-induced perturbations.

Mitochondrial ROS has been implicated in inflammasome activation (6). We found that basal ROS production as determined by the fluorescent dye CM-H₂DCFDA was lower in untreated or LPS-treated *Pgam5*^{-/-} BMDMs (Fig. 5A, 5B). Nigericin transiently

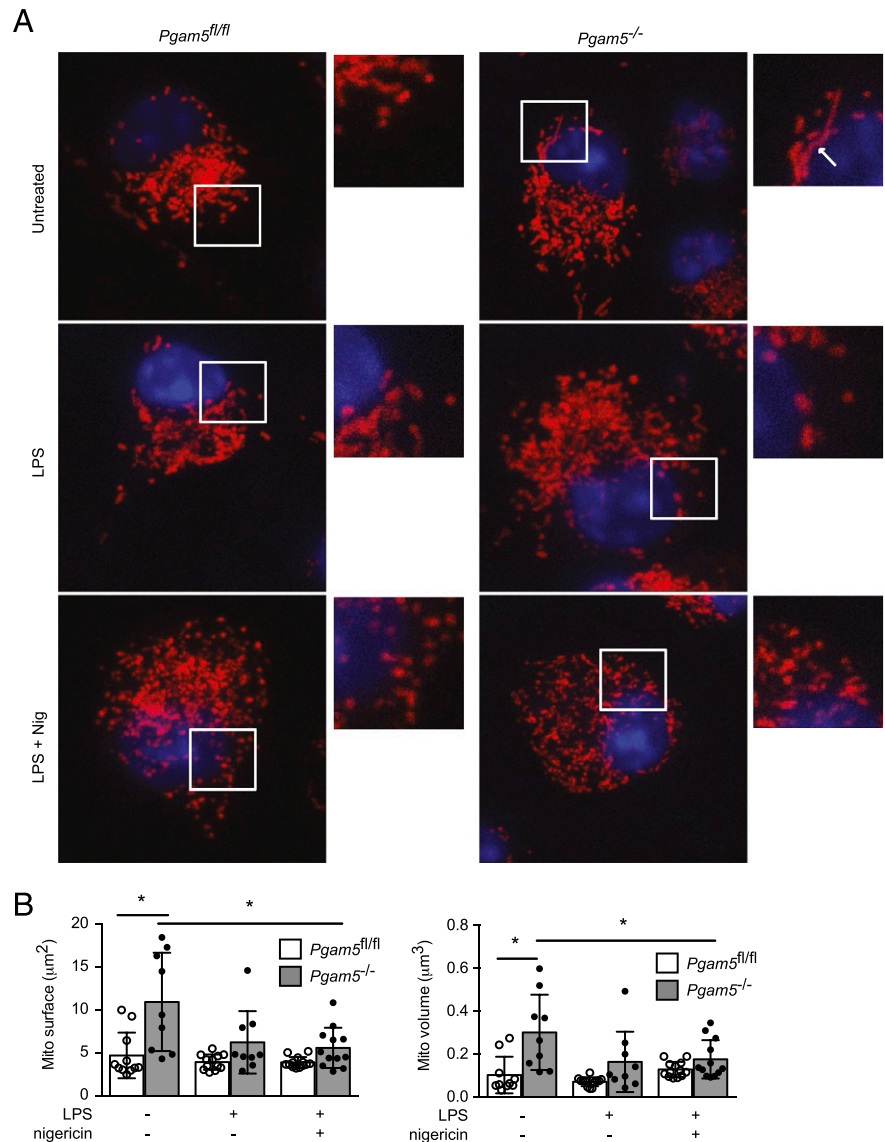


FIGURE 4. PGAM5 regulates mitochondrial homeostasis. **(A)** MitoTracker red staining of $Pgam5^{fl/fl}$ and $Pgam5^{-/-}$ BMDMs treated with LPS or LPS and nigericin. Red represents MitoTracker red; blue represents DAPI. Magnified versions of the indicated areas of interest are shown on the right. The white arrow in the inset shows an elongated mitochondria. **(B)** Mitochondrial surface and volume were quantified for $Pgam5^{fl/fl}$ and $Pgam5^{-/-}$ BMDMs using the 3D Object counter plugin for the Fiji software (version 2.0) and ImageJ as described in *Materials and Methods* (18). Results shown are mean \pm SEM. * $p \leq 0.05$.

increased ROS production in LPS-primed $Pgam5^{-/-}$ BMDMs to a level similar to that in $Pgam5^{fl/fl}$ BMDMs (Fig. 5A, 5B). However, by 30 min poststimulation, ROS level in $Pgam5^{-/-}$ BMDMs was again lower than that in $Pgam5^{fl/fl}$ BMDMs (Fig. 5A, 5B), although the difference was not statistically significant. These results suggest that $Pgam5^{-/-}$ BMDMs are defective in maintaining high levels of ROS production. Consistent with a role for ROS in IL-1 β processing, the antioxidant *N*-acetyl cysteine significantly reduced IL-1 β secretion by $Pgam5^{fl/fl}$ BMDMs, but not $Pgam5^{-/-}$ BMDMs (Fig. 5C). Furthermore, complete depolarization of the mitochondria by the uncoupler CCCP abrogated IL-1 β secretion in both $Pgam5^{fl/fl}$ and $Pgam5^{-/-}$ BMDMs (Fig. 5C). PGAM5 has been implicated to mediate mitochondria fission by dephosphorylating DRP1 at S637 (12). However, dephosphorylation of DRP1 at S637 in response to LPS and nigericin was similar in $Pgam5^{fl/fl}$

and $Pgam5^{-/-}$ BMDMs (Fig. 5D), suggesting that DRP1 is not a main target of PGAM5 in pro-IL-1 β processing.

PGAM5 and RIPK3 regulate IL-1 β secretion through distinct pathways

A recent study indicates that RIPK3 acts upstream of DRP-1 to promote dsRNA-induced IL-1 β secretion (16). However, BMDMs generated from *LysM-Cre;Drp1^{fl/fl}* or *Ripk3^{-/-}* mice do not exhibit defects in dsRNA-induced inflammasome activation (28). We therefore sought to clarify the relationship between RIPK3 and PGAM5 in inflammasome activation and IL-1 β secretion. We found that VSV-infected *Ripk3^{-/-}* BMDMs produced a normal level of IL-1 β (Fig. 5E). In addition, BMDMs derived from knock-in mice expressing kinase inactive RIPK1 (*Ripk1^{kd/kd}*) or RIPK3 (*Ripk3^{kd/kd}*) (33, 34) also produced normal levels of IL-1 β

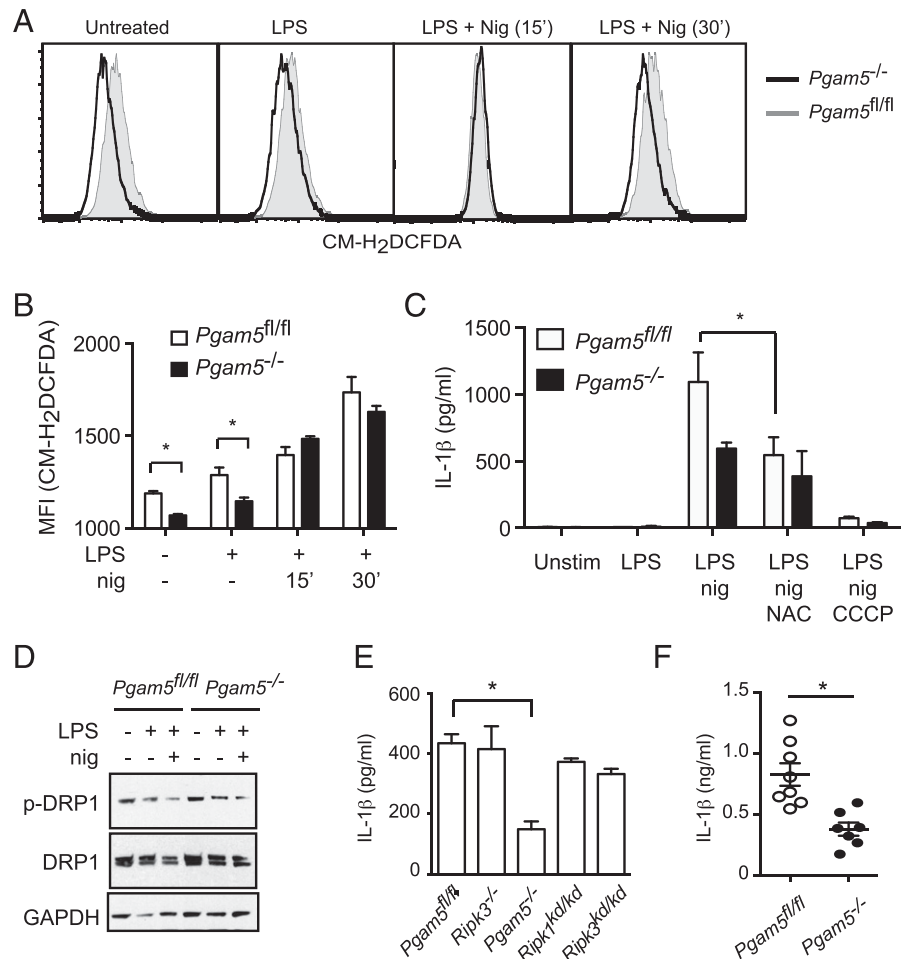


FIGURE 5. PGAM5, but not RIPK3, is required for VSV-induced IL-1 β secretion. **(A)** Untreated, LPS-treated, or LPS and nigericin-treated BMDMs from *Pgam5^{fl/fl}* (shaded curves) and *Pgam5^{-/-}* (black curves) mice were monitored for ROS production using the fluorescent probe CM-H₂DCFDA. **(B)** Mean fluorescence intensity (MFI) of CM-H₂DCFDA staining of BMDMs treated under the indicated conditions. **(C)** BMDMs were treated with LPS and nigericin as described in *Materials and Methods*. Where indicated, the cells were pretreated 20 mM *N*-acetyl cysteine (NAC) or 50 μ M CCCP for 30 min before addition of nigericin. IL-1 β secretion was measured 3 h after nigericin treatment. **(D)** BMDMs were treated with LPS for 3 h, followed by nigericin for 30 min. DRP1 phosphorylation at S637 was detected by Western blot as indicated. **(E)** LPS-primed BMDMs of the indicated genotypes were infected with VSV for 6 h. IL-1 β release was determined by ELISA. **(F)** *Pgam5^{fl/fl}* ($n = 8$) and *Pgam5^{-/-}* ($n = 7$) mice were injected i.p. with LPS and Alum for 2 h, and IL-1 β in the peritoneal exudate was determined by ELISA. Results shown are mean \pm SEM. * $p \leq 0.05$.

in response to VSV (Fig. 5E). By contrast, VSV-induced IL-1 β secretion was reduced in *Pgam5^{-/-}* BMDMs (Fig. 5E). Hence PGAM5 controls inflammasome activation and IL-1 β release in BMDMs independent of RIPK1 and RIPK3 function.

We next investigated whether PGAM5 is also required for IL-1 β release in vivo. Alum injection induces peritonitis and IL-1 β release in a NLRP3 inflammasome-dependent manner (35). In this model, *Pgam5^{-/-}* mice produced significantly reduced levels of IL-1 β compared with wild type mice (Fig. 5F), indicating that PGAM5 is also important for in vivo IL-1 β release.

Discussion

PGAM5 was originally identified as a mitochondrial phosphatase that controls cellular oxidative stress through binding to the Keap1-Nrf2 complex (9, 36). PGAM5 also binds to Bcl-X_L and thus can indirectly promote Bcl-X_L degradation and sensitize cells to apoptosis (11). In addition, cleaved PGAM5 was implicated in apoptosis (31, 37). In contrast with these proapoptotic functions, *Drosophila* PGAM5 was shown to protect against heat shock-induced apoptosis of the mushroom body (38). The role of PGAM5 in necroptosis is similarly confusing. Although it was first reported to be a key substrate of RIPK3 in necroptosis (12), subsequent shRNA knockdown studies did not reveal a prominent role for PGAM5 in necroptosis (14, 15). Using *Pgam5^{-/-}* MEFs and BMDMs, we definitively showed that PGAM5 is dispensable for apoptosis or necroptosis induced by multiple stimuli. This observation is surprising in light of the growth and survival defects of *Pgam5^{-/-}* mice. It is noteworthy that several recent reports have indicated a key role for PGAM5 in mitophagy (10, 11, 30).

Accumulation of damaged mitochondria in *Pgam5^{-/-}* mice might contribute to the growth and survival defects. Consistent with this notion, dopaminergic neurons were progressively lost in aging *Pgam5^{-/-}* mice (30).

Although PGAM5 is dispensable for cell death by apoptosis and necroptosis, it has a critical role in processing of pro-IL-1 β in BMDMs. IL-1 β is a key inflammatory cytokine with wide-ranging effects in immune responses and many inflammatory diseases. In this study, we showed that the mitochondrial phosphatase PGAM5 is dispensable for necroptosis and apoptosis, but has a crucial role in optimal IL-1 β secretion by BMDMs in response to multiple inflammasome agonists. This effect is achieved through caspase 1-mediated cleavage of pro-IL-1 β , because inflammasome assembly was severely impaired in *Pgam5^{-/-}* BMDMs. PGAM5 likely controls inflammasome activation indirectly, because we did not detect direct physical interaction between PGAM5 and ASC (data not shown). However, PGAM5 was found in the same detergent-insoluble compartment as the inflammasome. Unlike ASC, which translocated only to the detergent-insoluble compartment in response to nigericin, LPS alone triggered PGAM5 translocation to this compartment. PGAM5 accumulation and oligomerization in this compartment was further enhanced by nigericin. Mitochondria-produced ROS has been implicated in inflammasome activation (6). Consistent with PGAM5's proposed role in mitochondrial fission, the mitochondria in *Pgam5^{-/-}* BMDMs were elongated with increased volume and surface. *Pgam5^{-/-}* BMDMs underwent mitochondrial fragmentation in response to LPS, suggesting that PGAM5 has important functions in maintaining mitochondrial homeostasis. Consistent with this

notion, we found that *Pgam5*^{-/-} BMDMs were impaired in ROS production. However, the effect of PGAM5 deficiency on LPS and nigericin-induced ROS production was modest and not statistically significant. This suggests that other mechanisms might be involved in PGAM5-mediated inflammasome activation.

Emerging evidence indicates that cell death signal adaptors often have dual roles in inflammation (39, 40). In particular, the apoptosis adaptors FADD and caspase 8, and the necroptosis adaptors RIPK1 and RIPK3, can regulate inflammasome activity in both BMDMs and BMDCs (13, 17, 27, 28). The mechanism used by these cell death adaptors to control pro-IL-1 β processing varies greatly depending on the cell type and stimulus used. For example, caspase 8 can complex with FADD, RIPK1, and RIPK3 to directly cleave pro-IL-1 β . When caspase 8 activity is inhibited, this complex can, in turn, recruit MLKL to promote IL-1 β maturation through a yet to be defined mechanism (27, 28). Interestingly, RIPK3 was reported to stimulate NLRP3 inflammasome activation via PGAM5 in caspase 8-deficient dendritic cells (13). In wild type BMDMs, however, we found that PGAM5, but not RIPK3, was required for optimal inflammasome activation and VSV-induced IL-1 β secretion by BMDMs. This is in contrast with a recent report, which showed that RIPK3, but not PGAM5, has an essential role in RNA virus-induced IL-1 β secretion in LPS-primed BMDMs (16). The reason for these discrepant observations is unknown at present, but may be related to efficiency of shRNA knockdown of PGAM5 in different studies. Rather, our results are consistent with a more recent report showing that RIPK3 is dispensable for dsRNA or VSV-induced inflammasome activation (28). Nonetheless, the inflammasome-stimulating activity of RIPK3 is unleashed regardless of the cell type used when cellular IAPs, FADD, or caspase 8 are inhibited (27). Under these conditions, RIPK3 and PGAM5 may cooperate with each other to stimulate inflammasome activity and pro-IL-1 β processing. Because PGAM5 facilitates activation of multiple inflammasomes, it will be interesting to determine whether targeting PGAM5 is a viable therapeutic strategy in IL-1 β -driven inflammatory diseases.

Acknowledgments

We thank Stephen Jones for providing the flippase and Cre deleter mice.

Disclosures

J.B. and P.J.G. are employees of GlaxoSmithKline. The other authors have no financial conflicts of interest.

References

- Lamkanfi, M., and V. M. Dixit. 2014. Mechanisms and functions of inflammasomes. *Cell* 157: 1013–1022.
- Lu, A., V. G. Magupalli, J. Ruan, Q. Yin, M. K. Atianand, M. R. Vos, G. F. Schröder, K. A. Fitzgerald, H. Wu, and E. H. Egelman. 2014. Unified polymerization mechanism for the assembly of ASC-dependent inflammasomes. *Cell* 156: 1193–1206.
- Cai, X., J. Chen, H. Xu, S. Liu, Q. X. Jiang, R. Halfmann, and Z. J. Chen. 2014. Prion-like polymerization underlies signal transduction in antiviral immune defense and inflammasome activation. *Cell* 156: 1207–1222.
- Moriwaki, K., J. Bertin, P. J. Gough, and F. K. Chan. 2015. A RIPK3-caspase 8 complex mediates atypical pro-IL-1 β processing. *J. Immunol.* 194: 1938–1944.
- Gurung, P., J. R. Lukens, and T. D. Kanneganti. 2015. Mitochondria: diversity in the regulation of the NLRP3 inflammasome. *Trends Mol. Med.* 21: 193–201.
- Zhou, R., A. S. Yazdi, P. Menu, and J. Tschopp. 2011. A role for mitochondria in NLRP3 inflammasome activation. *Nature* 469: 221–225.
- Nakahira, K., J. A. Haspel, V. A. Rathinam, S. J. Lee, T. Dolinay, H. C. Lam, J. A. Englert, M. Rabinovitch, M. Cernadas, H. P. Kim, et al. 2011. Autophagy proteins regulate innate immune responses by inhibiting the release of mitochondrial DNA mediated by the NALP3 inflammasome. *Nat. Immunol.* 12: 222–230.
- Shimada, K., T. R. Crother, J. Karlin, J. Dagvadorj, N. Chiba, S. Chen, V. K. Ramanujan, A. J. Wolf, L. Vergnes, D. M. Ojcius, et al. 2012. Oxidized mitochondrial DNA activates the NLRP3 inflammasome during apoptosis. *Immunity* 36: 401–414.
- Lo, S. C., and M. Hannink. 2006. PGAM5, a Bcl-XL-interacting protein, is a novel substrate for the redox-regulated Keap1-dependent ubiquitin ligase complex. *J. Biol. Chem.* 281: 37893–37903.
- Chen, G., Z. Han, D. Feng, Y. Chen, L. Chen, H. Wu, L. Huang, C. Zhou, X. Cai, C. Fu, et al. 2014. A regulatory signaling loop comprising the PGAM5 phosphatase and CK2 controls receptor-mediated mitophagy. *Mol. Cell* 54: 362–377.
- Wu, H., D. Xue, G. Chen, Z. Han, L. Huang, C. Zhu, X. Wang, H. Jin, J. Wang, Y. Zhu, et al. 2014. The BCL2L1 and PGAM5 axis defines hypoxia-induced receptor-mediated mitophagy. *Autophagy* 10: 1712–1725.
- Wang, Z., H. Jiang, S. Chen, F. Du, and X. Wang. 2012. The mitochondrial phosphatase PGAM5 functions at the convergence point of multiple necrotic death pathways. *Cell* 148: 228–243.
- Kang, T. B., S. H. Yang, B. Toth, A. Kovalenko, and D. Wallach. 2013. Caspase-8 blocks kinase RIPK3-mediated activation of the NLRP3 inflammasome. *Immunity* 38: 27–40.
- Murphy, J. M., P. E. Czabotar, J. M. Hildebrand, I. S. Lucet, J. G. Zhang, S. Alvarez-Diaz, R. Lewis, N. Lalouji, D. Metcalf, A. I. Webb, et al. 2013. The pseudokinase MLKL mediates necroptosis via a molecular switch mechanism. *Immunity* 39: 443–453.
- Remijsen, Q., V. Goossens, S. Grootjans, C. Van den Haute, N. Vanlangenakker, Y. Dondelinger, R. Roelandt, I. Bruggeman, A. Goncalves, M. J. Bertrand, et al. 2014. Depletion of RIPK3 or MLKL blocks TNF-driven necroptosis and switches towards a delayed RIPK1 kinase-dependent apoptosis. *Cell Death Dis.* 5: e1004.
- Wang, X., W. Jiang, Y. Yan, T. Gong, J. Han, Z. Tian, and R. Zhou. 2014. RNA viruses promote activation of the NLRP3 inflammasome through a RIP1-RIP3-DRP1 signaling pathway. *Nat. Immunol.* 15: 1126–1133.
- Moriwaki, K., S. Balaji, T. McQuade, N. Malhotra, J. Kang, and F. K. Chan. 2014. The necroptosis adaptor RIPK3 promotes injury-induced cytokine expression and tissue repair. *Immunity* 41: 567–578.
- Bolte, S., and F. P. Cordelières. 2006. A guided tour into subcellular colocalization analysis in light microscopy. *J. Microsc.* 224: 213–232.
- Takeda, K., Y. Komuro, T. Hayakawa, H. Oguchi, Y. Ishida, S. Murakami, T. Noguchi, H. Kinoshita, Y. Sekine, S. Iemura, et al. 2009. Mitochondrial phosphoglycerate mutase 5 uses alternate catalytic activity as a protein serine/threonine phosphatase to activate ASK1. *Proc. Natl. Acad. Sci. USA* 106: 12301–12305.
- Ramachandran, A., M. R. McGill, Y. Xie, H. M. Ni, W. X. Ding, and H. Jaeschke. 2013. Receptor interacting protein kinase 3 is a critical early mediator of acetaminophen-induced hepatocyte necrosis in mice. *Hepatology* 58: 2099–2108.
- He, S., Y. Liang, F. Shao, and X. Wang. 2011. Toll-like receptors activate programmed necrosis in macrophages through a receptor-interacting kinase-3-mediated pathway. *Proc. Natl. Acad. Sci. USA* 108: 20054–20059.
- Kaiser, W. J., J. W. Upton, A. B. Long, D. Livingston-Rosanoff, L. P. Daley-Bauer, R. Hakem, T. Caspary, and E. S. Mocarski. 2011. RIP3 mediates the embryonic lethality of caspase-8-deficient mice. *Nature* 471: 368–372.
- Oberst, A., C. P. Dillon, R. Weinlich, L. L. McCormick, P. Fitzgerald, C. Pop, R. Hakem, G. S. Salvesen, and D. R. Green. 2011. Catalytic activity of the caspase-8-FLIP(L) complex inhibits RIPK3-dependent necrosis. *Nature* 471: 363–367.
- Zhang, H., X. Zhou, T. McQuade, J. Li, F. K. Chan, and J. Zhang. 2011. Functional complementation between FADD and RIP1 in embryos and lymphocytes. *Nature* 471: 373–376.
- Dillon, C. P., A. Oberst, R. Weinlich, L. J. Janke, T. B. Kang, T. Ben-Moshe, T. W. Mak, D. Wallach, and D. R. Green. 2012. Survival function of the FADD-CASPASE-8-cFLIP(L) complex. *Cell Reports* 1: 401–407.
- Dillon, C. P., R. Weinlich, D. A. Rodriguez, J. G. Cripps, G. Quarato, P. Gurung, K. C. Verbist, T. L. Brewer, F. Llambi, Y. N. Gong, et al. 2014. RIPK1 blocks early postnatal lethality mediated by caspase-8 and RIPK3. *Cell* 157: 1189–1202.
- Lawlor, K. E., N. Khan, A. Mildenhall, M. Gerlic, B. A. Croker, A. A. D'Cruz, C. Hall, S. Kaur Spall, H. Anderton, S. L. Masters, et al. 2015. RIPK3 promotes cell death and NLRP3 inflammasome activation in the absence of MLKL. *Nat. Commun.* 6: 6282.
- Kang, S., T. Fernandes-Alnemri, C. Rogers, L. Mayes, Y. Wang, C. Dillon, L. Roback, W. Kaiser, A. Oberst, J. Sagara, et al. 2015. Caspase-8 scaffolding function and MLKL regulate NLRP3 inflammasome activation downstream of TLR3. *Nat. Commun.* 6: 7515.
- Yu, J. W., T. Fernandes-Alnemri, P. Datta, J. Wu, C. Juliana, L. Solorzano, M. McCormick, Z. Zhang, and E. S. Alnemri. 2007. Pyrin activates the ASC proteasome in response to engagement by autoinflammatory PSTPIP1 mutants. *Mol. Cell* 28: 214–227.
- Lu, W., S. S. Karuppagounder, D. A. Springer, M. D. Allen, L. Zheng, B. Chao, Y. Zhang, V. L. Dawson, T. M. Dawson, and M. Lenardo. 2014. Genetic deficiency of the mitochondrial protein PGAM5 causes a Parkinson's-like movement disorder. *Nat. Commun.* 5: 4930.
- Sekine, S., Y. Kanamaru, M. Koike, A. Nishihara, M. Okada, H. Kinoshita, M. Kamiyama, J. Maruyama, Y. Uchiyama, N. Ishihara, et al. 2012. Rhomboid protease PARL mediates the mitochondrial membrane potential loss-induced cleavage of PGAM5. *J. Biol. Chem.* 287: 34635–34645.
- Imai, Y., T. Kanao, T. Sawada, Y. Kobayashi, Y. Moriwaki, Y. Ishida, K. Takeda, H. Ichijo, B. Lu, and R. Takahashi. 2010. The loss of PGAM5 suppresses the mitochondrial degeneration caused by inactivation of PINK1 in *Drosophila*. *PLoS Genet.* 6: e1001229.

33. Berger, S., V. Kasparcova, S. Hoffman, B. Swift, L. Dare, M. Schaeffer, C. Capriotti, M. Cook, J. Finger, A. Hughes-Earle, et al. 2014. Cutting edge: RIP1 kinase activity is dispensable for normal development but is a key regulator of inflammation in SHARPIN-deficient mice. *J Immunol.* 192: 5476–5480.
34. Mandal, P., S. B. Berger, S. Pillay, K. Moriwaki, C. Huang, H. Guo, J. D. Lich, J. Finger, V. Kasparcova, B. Votta, et al. 2014. RIP3 induces apoptosis independent of pronecrotic kinase activity. *Mol. Cell* 56: 481–495.
35. Eisenbarth, S. C., O. R. Colegio, W. O'Connor, F. S. Sutterwala, and R. A. Flavell. 2008. Crucial role for the Nalp3 inflammasome in the immunostimulatory properties of aluminium adjuvants. *Nature* 453: 1122–1126.
36. Lo, S. C., and M. Hannink. 2008. PGAM5 tethers a ternary complex containing Keap1 and Nrf2 to mitochondria. *Exp. Cell Res.* 314: 1789–1803.
37. Zhuang, M., S. Guan, H. Wang, A. L. Burlingame, and J. A. Wells. 2013. Substrates of IAP ubiquitin ligases identified with a designed orthogonal E3 ligase, the NEDDylator. *Mol. Cell* 49: 273–282.
38. Ishida, Y., Y. Sekine, H. Oguchi, T. Chihara, M. Miura, H. Ichijo, and K. Takeda. 2012. Prevention of apoptosis by mitochondrial phosphatase PGAM5 in the mushroom body is crucial for heat shock resistance in *Drosophila melanogaster*. *PLoS One* 7: e30265.
39. Chan, F. K., N. F. Luz, and K. Moriwaki. 2015. Programmed necrosis in the cross talk of cell death and inflammation. *Annu. Rev. Immunol.* 33: 79–106.
40. Silke, J., J. A. Rickard, and M. Gerlic. 2015. The diverse role of RIP kinases in necroptosis and inflammation. *Nat. Immunol.* 16: 689–697.